Journal of Membrane Science 341 (2009) 67–75

Contents lists available at ScienceDirect

Journal of Membrane Science

journal homepage: www.elsevier.com/locate/memsci

Preparation, characterization and performance of Al_2O_3/PES membrane for wastewater filtration

Nermen Maximous, G. Nakhla*, W. Wan, K. Wong

Department of Chemical and Biochemical Engineering, Faculty of Engineering, University of Western Ontario, 1151 Richmond Street, London, Ont., Canada N6A 5B9

ARTICLE INFO

Article history:
Received 16 April 2009
Received in revised form 26 May 2009
Accepted 26 May 2009
Available online 23 June 2009

Keywords:
Al_2O_3
Nanoparticle
Membrane bioreactor
Fouling mitigation
Activated sludge

ABSTRACT

Membrane bioreactors (MBRs) have been widely used as advanced wastewater treatment processes in recent years. However, membrane fouling and its consequences in terms of plant maintenance and operating costs limit the widespread application of MBRs. Thus great efforts have focused on fouling mitigation. In this study, Al_2O_3 entrapped polyethersulfone (PES) ultrafiltration membranes were prepared and applied to activated sludge filtration in order to evaluate their fouling characteristics. The impact of solvent evaporation time and polymer concentrations on ultrafiltration (UF) membrane characteristics and performance was studied. PES was employed as a base polymer, while *N*-methyl pyrrolidone (NMP) was used as a solvent. The flat sheet membranes, prepared via phase inversion, were characterized using scanning electron microscope (SEM). Membrane performance was changed by the addition of Al_2O_3 nanoparticles to the casting solution. Al_2O_3 entrapped membrane showed lower flux decline compared to that of neat polymeric membrane. Fouling mitigation effect increased with nanoparticle content. No significant effect of the nanoparticles distribution pattern inside the membrane matrix was found on the membrane performance. This study highlights the potential of Al_2O_3 immobilized membranes in MBR application.

1. Introduction

The MBR process has now become an attractive option for the treatment and reuse of industrial and municipal wastewaters. However, the MBR filtration performance inevitably decreases with filtration time due to membrane fouling. More severe fouling is expected when hydrophobic membranes are used in the MBR. Polyethersulfone (PES) has become an important separation membrane material, as it possesses many good physical and chemical characteristics such as good heat-aging resistance and environmental endurance as well as easy processing. However, the inherent hydrophobicity of PES due to its structure leads to a low membrane flux and poor anti-fouling properties, which have a great impact on its application and useful life [1]. Therefore, efforts have focused on increasing PES hydrophilicity either by chemical or physical modifications such as ultraviolet irradiation [2], blending with hydrophilic materials [3], graft polymerization [4], plasma graft [5], and so on. Of the aforementioned methods, blending with inorganic materials, especially nanoparticles, has attracted much interest due to their convenient operation and mild conditions [6]. Moreover, by the way of blending, the modified membrane can combine basic properties of organic and inorganic materials and offer specific advantages for the preparation of artificial membranes with excellent separation performances, good thermal and chemical resistance and adaptability to the harsh wastewater environments [7–10]. Several types of inorganic materials have been blended with polyvinylidene fluoride (PVDF) such as silica [11], zirconium dioxide (ZrO_2) [12], Al_2O_3 [13] and some low molecular weight inorganic salts, such as lithium salts [14]. TiO_2 nanoparticles have also been used in water treatment membrane technology in recent years [8–10]. Molinari et al. [8–10] who tried to report on the promise of photocatalytic membrane reactor for toxic organic removal [8–10], immobilize TiO_2 nanoparticles on flat polymeric ultrafiltration (UF) membranes in two different ways. TiO_2/polymer thin film composite (TFC) reverse osmosis membrane has been investigated to mitigate biofouling by photobactericidal effect under ultraviolet (UV) radiation [15,16]. Bae and Tak [17] investigated the fouling mitigation effect of immobilized TiO_2 UF membranes during the activated sludge filtration. However, studies of blending membranes with nanoparticles focused primarily on gas separation [18–20] and pervaporation membranes [21–23] and have recently been extended to porous membranes for ultrafiltration (especially PVDF membranes) [11–14] and potential nanofiltration applications [24].

Since, no studies have been conducted on Al_2O_3 immobilized membranes for activated sludge filtration despite previous applications in water treatment [13], the novelty in this research lies in introducing Al_2O_3 nanoparticles to PES in order to improve the

* Corresponding author. Tel.: +1 519 661 2111x85470; fax: +1 519 850 2921.
E-mail addresses: nmaximou@uwo.ca (N. Maximous), gnakhla@eng.uwo.ca (G. Nakhla), wkwan@eng.uwo.ca (W. Wan), khwong@uwo.ca (K. Wong).

0376-7388/$ – see front matter © 2009 Elsevier B.V. All rights reserved.
doi:10.1016/j.memsci.2009.05.040

performance of PES membrane for wastewater filtration. Therefore, this research aimed to prepare pure PES membrane and Al_2O_3–PES composite membranes using the phase inversion method by including a small proportion of Al_2O_3 particles to the casting solution. The effects of polymer preparation conditions such as polymer concentration, solvent evaporation time and Al_2O_3-particle concentration in the casting solution on the membrane permeation flux were studied. The membranes morphology was characterized by SEM. Investigation of the fouling mitigation effect of Al_2O_3 immobilized UF membranes during the activated sludge filtration was also included in this study.

2. Experimental

2.1. Membrane preparation

Pure PES flat membranes were prepared by phase inversion [25]. PES Radel A-100 (Solvay Advanced Polymers, Alpharetta, GA, USA) was used as membrane material. NMP solvent was selected in the current study as it is widely accepted as a good solvent for many polymers [11,12,17]. The effect of polymer concentration was tested by preparing casting solutions consisting of 5, 10, 15, 18 and 20 wt%, PES polymer and NMP (Sigma–Aldrich Canada Ltd.). The membranes were casted with a 100 μm casting knife onto a glass plate at room temperature; the nascent membrane was evaporated at 25 ± 1 °C for 30 s then immersed in a deionized water coagulation bath maintained at 18 ± 1 °C for 2 min. In order to study the effect of solvent evaporation time on membrane preparation, the 18 wt% nascent membranes were casted by the same method described above and evaporated at 25 ± 1 °C for 15, 30, 60 and 120 s.

For the entrapped membrane 0.01, 0.03, 0.05 Al_2O_3/PES mass ratios were prepared. Al_2O_3 nanoparticles with average particle size of 48 nm and a surface area of 34 m^2/g (Sigma–Aldrich Canada Ltd.) were dissolved into the NMP solution and was sonicated at 60 °C for 72 h to obtain a uniform and homogeneous casting suspension. Subsequently, 18 wt% polymer was added and the mixture was sonicated again for a week, the membranes were cast with a 100 μm casting knife onto a glass plate at room temperature. The nascent membrane was evaporated at 25 ± 1 °C for 15 s and then immersed in a deionized water coagulation bath maintained at 18 ± 1 °C for 2 min. For all prepared membranes, after complete coagulation, the membrane was transferred to a water bath for 15–17 days at room temperature to remove the remaining solvent from the membrane structure before it testing.

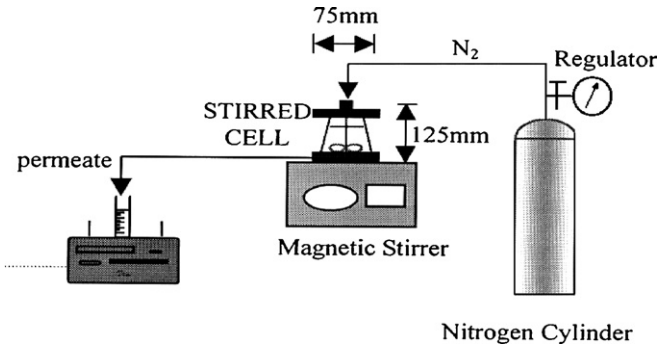

Fig. 1. Schematic diagram of stirred batch cell system.

2.2. Membrane characterization

In order to operate under constant trans-membrane pressure (TMP), membrane filtration was carried out using a stirred batch cell (Model No. 8050, Amicon) as shown in (Fig. 1). The mode of constant TMP is suitable for the study of membrane fouling and there are still many reports about the application of constant TMP for long-term wastewater treatment [26–29]. The deionized water (DIW) flux was determined for the PES control membranes as well as the Al_2O_3 entrapped PES at different TMPs of 0.345, 0.69, 1.034, 1.38 and 1.724 bar). The cross-sectional morphologies of the membranes were characterized using SEM (Leo 1530, LEO Electron Microscopy Ltd) at 1 kV with no conductive coating. To expose the cross-section for SEM characterization, the membranes were cryogenically fractured in liquid nitrogen. The distribution of the Al_2O_3 nanoparticles and the dimension of the membranes were measured using the Java-based image processing program, Image J (National Institutes of Health).

2.3. Activated sludge

Activated sludge used in this study was cultivated in a submerged laboratory scale MBR (Fig. 2) treating synthetic wastewater for more than 5 months. Starch and casein, $(NH_4)_2SO_4$, and KH_2PO_4 were used as carbon, nitrogen and phosphorus sources, respec-

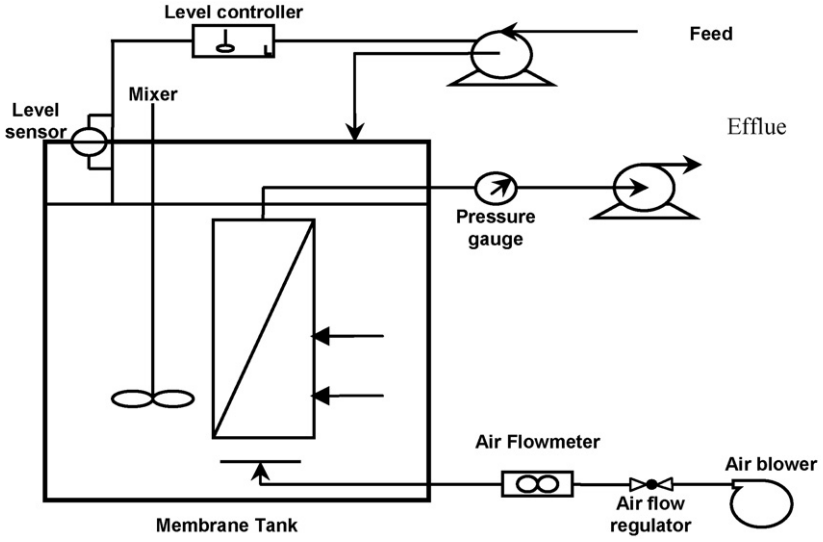

Fig. 2. Schematic diagram of MBR experimental setup.

Table 1
Feed composition.

Compound	Concentration (mg/L)
Casein	125
Starch	84.4
Sodium acetate	31.9
$(NH_4)_2SO_4$	93.0
$MgSO_4{\cdot}7H_2O$	69.6
$CaCl_2{\cdot}2H_2O$	22.5
K_2HPO_4	5.9
NaOH	175.0
$FeCl_3$	11.0
$CuSO_4{\cdot}4H_2O$	0.08
$NaMoO_4{\cdot}2H_2O$	0.15
$MnSO_4{\cdot}H_2O$	0.13
$ZnCl_2$	0.23
$CoCl_2{\cdot}6H_2O$	0.42
KH_2PO_4	23.6
Na_2CO_3	216
$NaHCO_3$	169

tively. Additional nutrients and alkalinity ($NaHCO_3$) were also supplied to the reactor. The feed composition and the sludge characteristics are summarized in Tables 1 and 2, respectively.

2.4. Membrane fouling analysis

Since new polymeric membrane can be compacted by applied pressure during the filtration, the flux can decline without membrane fouling. In order to alleviate the impact of compaction on flux, pre-filtration studies with pure deionized water (DIW) were conducted until a steady-state flux (J_{iw}) was achieved. For sludge filtration, the TMP and stirring speed were kept constant at 0.69 bar (as this is a typical TMP for submerged membranes like Zenon [30]) and 600 rpm, respectively. The permeate flux was determined by monitoring the volume of permeate with time. After the filtration test, the membrane was washed in a cross-flow manner with DIW, the pure DIW flux (J_{fw}) was measured four times after this cleaning regime.

The degree of membrane fouling was calculated quantitatively using the resistance-in-series model [31]

$$J = \frac{\text{TMP}}{\eta R_t}$$

where J = the flux (L/m^2 h); TMP = trans-membrane pressure (1.03 bar); η = viscosity of water at room temperature.

$$R_t = R_m + R_f + R_c$$

Resistances values were obtained by the following equations

$$R_m = \frac{\text{TMP}}{\eta J_{iw}}$$

$$R_f = \frac{\text{TMP}}{\eta J_{fw}} - R_m$$

$$R_c = \frac{\text{TMP}}{\eta J} - (R_m + R_f)$$

Table 2
Sludge characteristics.

Parameters	Average ± SD
TSS (g/L)	8.07 ± 1.1
VSS (g/L)	5.89 ± 1.1
SCOD (mg/L)	22.4 ± 2.0
TCOD (mg/L)	363.3 ± 33.5
NO_3 ($mgNO_3$-N/L)	7.5 ± 1.6
NH_3 ($mgNH_3$-N/L)	1.10 ± 0.57
PO_4($mgPO_4$-P/L)	5.6 ± 1.3
pH	7.3 ± 0.2
DO	4.2 ± 0.8

where R_m is the intrinsic membrane resistance; R_f is the sum of the resistances caused by solute adsorption into the membrane pores or walls and chemically reversible cake. R_c is the cake resistance formed by cake layer deposited over the membrane surface.

3. Results and discussion

3.1. Membrane preparation conditions

3.1.1. Polymer concentration

Polymer concentration has been identified as the most important parameter for tailoring membrane properties [32]. Table 3 shows the effect of different polymer concentrations on the membrane DIW permeation. The membranes were cast at a constant solvent evaporation time of 30 s. It has been generally accepted as a common rule that thermodynamically less stable membrane forming systems can enhance the precipitation rate and make more porous membranes and vice versa [32]. Thus, in this phase of study all the new developed doping solutions were designed specifically to be thermodynamically less stable in order to increase the membrane porosity. As shown in Table 3, as the polymer concentration increased the DIW permeation of the membrane decreased and the pressure resistance increased. This suggests that increasing polymer concentration will form a denser and thicker skin layer, resulting in higher pressure resistance, but less productive asymmetric ultrafiltration membranes for liquid separation. Higher polymer concentrations are required to induce chain entanglement and therefore reduce the formation of macro-voids in the skin layer [32]. As a result, the separation capability of the membrane will increase but the permeability will decline. The membranes with 5 wt% polymer concentrations were transparent and very sensitive to dehydration; they shrank very easily upon drying. On the other hand, the membranes with 20 wt% polymer concentration were impermeable to water at the tested TMP. Membranes with a dense and thick skin as well as porous structure were prepared with 18 wt% PES. Asymmetric membranes from the dilute polymer solution (10 and 15 wt%) produced a thin and porous skin layer, leading to a high flux but a relatively low pressure resistance. Pesek and Koros [33] who had investigated the effects of polymer concentration and solvent ratio on the membrane morphology and separation performance showed that increase in polymer concentration at constant solvent ratio, produced higher solution viscosities and selectivity but generally lower pressure-normalized fluxes. The aforementioned authors attributed flux losses to thicker skins and transition layers, believed to be caused by the slower re-dissolution of the polymer solution. On the other hand, simultaneous increases in polymer concentration and solvent ratios allow higher viscosity with little change in membrane performance. Since the addition of the nanoparticles with their hydrophilic nature might increase the membrane porosity and subsequently change the membrane pressure resistance, the 18 wt% which established the highest pressure resistance (Table 3) was selected to be the polymer concentration for the current study.

Table 3
The effect of polymer concentration on the membrane DIW permeation[a].

Polymer concentration	DIW permeation (L/m^2 bar-h)[b]	Max. sustained TMP (bar)
10 wt%	1227.4 ± (103)	1.034
15 wt%	1134.5 ± (111)	1.034
18 wt%	866.5 ± (59.6)	1.724

[a] All membranes were cast at constant solvent evaporation time of 30 s.

[b] The values presented in this table are the slopes of the straight lines generated by recording the DIW flux at different TMP. Numbers within parenthesis represent the 95% confidence intervals.

Table 4
The effect of solvent evaporation time on the membrane DIW permeation.

Solvent evaporation time (s)	DIW permeation (L/m^2 bar-h)[a]
15	866.5 ± (59.6)
30	343 ± (17.5)
60	294.5 ± (26.5)
120	10.7 ± (1.5)

[a] The values presented in this table are the slopes of the straight lines generated by recording the DIW flux at different TMP. Numbers within parenthesis represent the 95% confidence intervals.

Table 5
The effect of Al_2O_3 Nanoparticles concentration on the membrane DIW permeation.

Al_2O_3/PES ratios	DIW permeation (L/m^2 bar-h)[a]
0.01	1016 ± (38)
0.03	1026 ± (18)
0.05	1268 ± (35)

[a] The values presented in this table are the slopes of the straight lines generated by recording the DIW flux at different TMP. Numbers within parenthesis represent the 95% confidence intervals.

3.1.2. Solvent evaporation time

The second important factor that affects the membrane preparation and performance is the solvent evaporation time. Table 4 shows the effect of different evaporation times on the PES membrane DIW permeation. All the membranes were cast with 18 wt% polymer solution. The results showed that as the solvent evaporation time increases, the membrane DIW permeation decreases, potentially attributable to the decrease in the membrane pore size. The changes in membrane DIW were very drastic when evaporation time increased from 15 s (850.6 L/m^2 bar-h) to 120 s (10.7 L/m^2 bar-h) which suggested that within the range of evaporation times investigated in this study, the optimum solvent evaporation time is 15 s. The effect of evaporation time on the water permeation has been observed in numerous studies, including polysulfone membranes [34], for polyetheramide hydrazide polymer with a novel solvent exchange technique [35], and with a poly(phtalazine ether sulfone ketone) membrane [36]. Although the base polymer and the membrane preparation techniques were different, all of them observed a decrease of the water permeation rate with an increase in the solvent evaporation period.

3.1.3. Al_2O_3-content

The effect of Al_2O_3 nanoparticles concentrations was also studied. Table 5 shows the Al_2O_3-entrapped PES membranes DIW permeation. All the membranes were cast from 18 wt% PES solution with a solvent evaporation time of 15 s. As apparent from the table, membrane DIW permeation marginally increased as the nanoparticles concentration in the casting solution increased. Since Al_2O_3 has higher affinity for water than PES, penetration velocity of water into nascent membrane increased with Al_2O_3 concentration during the phase inversion. In addition, solvent diffusion from the membrane to the water can also be increased by Al_2O_3 addition. Since the interaction between polymer and solvent molecules decreased due to the hindrance of nanoparticles [37], solvent molecules could diffuse more easily from the polymer matrix. It is well known that both pore size and porosity increase with solvent interdiffusion velocity from the enriched gas as a result of evaporation to the liquid [37]. Thus, pore size and porosity of Al_2O_3-entrapped membrane could be slightly higher than those of neat PES membrane.

3.2. Membrane characterization

Fig. 3 showing the SEM picture for the PES membrane clearly indicates asymmetry and porosity. The Al_2O_3 nanoparticles distribution pattern inside the membrane matrix was also investigated in this work. For the 0.0 Al_2O_3/PES membrane, the inorganic nanoparticles load was too small to draw any conclusions. Figs. 4 and 5 show the Al_2O_3 distribution pattern for the 0.03 and 0.05 Al_2O_3/PES membranes with respect to membrane cross-section with areas of 351 and 651.9 μm^2, respectively. As apparent from the two figures, most of the Al_2O_3 particles are located between 0 and 30 μm of the membrane thickness and they significantly decreased after that depth. For the 0.03 Al_2O_3/PES membranes, the Al_2O_3 particles are uniformly distributed with about 25% of the particles in each 10 μm of membrane thickness. On the other hand, in the 0.05 Al_2O_3/PES membranes, 42% of the particles are located at 20–30 μm of membrane thickness. The ratio between the overall particle density for the 0.03 and 0.05 Al_2O_3/PES is 0.42 which is very close to the ratio of the particle density for the same membranes for the depth of 0–20 μm which is 0.5. The ratio between 0.03 and 0.05 Al_2O_3/PES fouling resistance (R_f), as discussed in Section 3.3.2, is 0.68 which is much greater than the 0.42–0.5 particle density, which coupled with the observation that the R_f values for 0.01 and 0.05 Al_2O_3 were

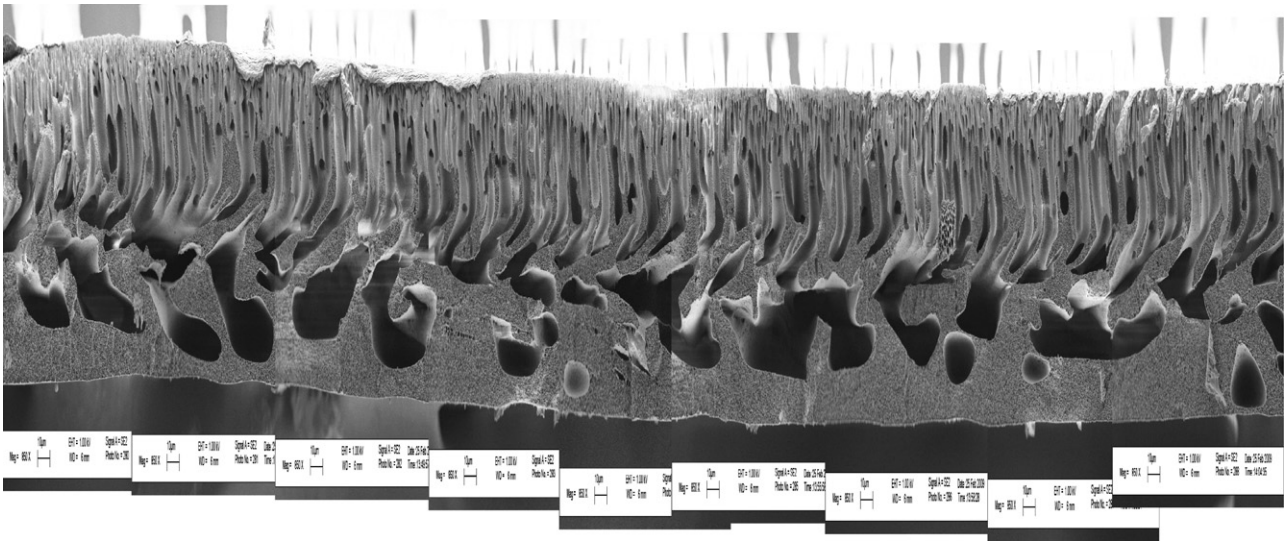

Fig. 3. SEM picture for the neat PES membrane.

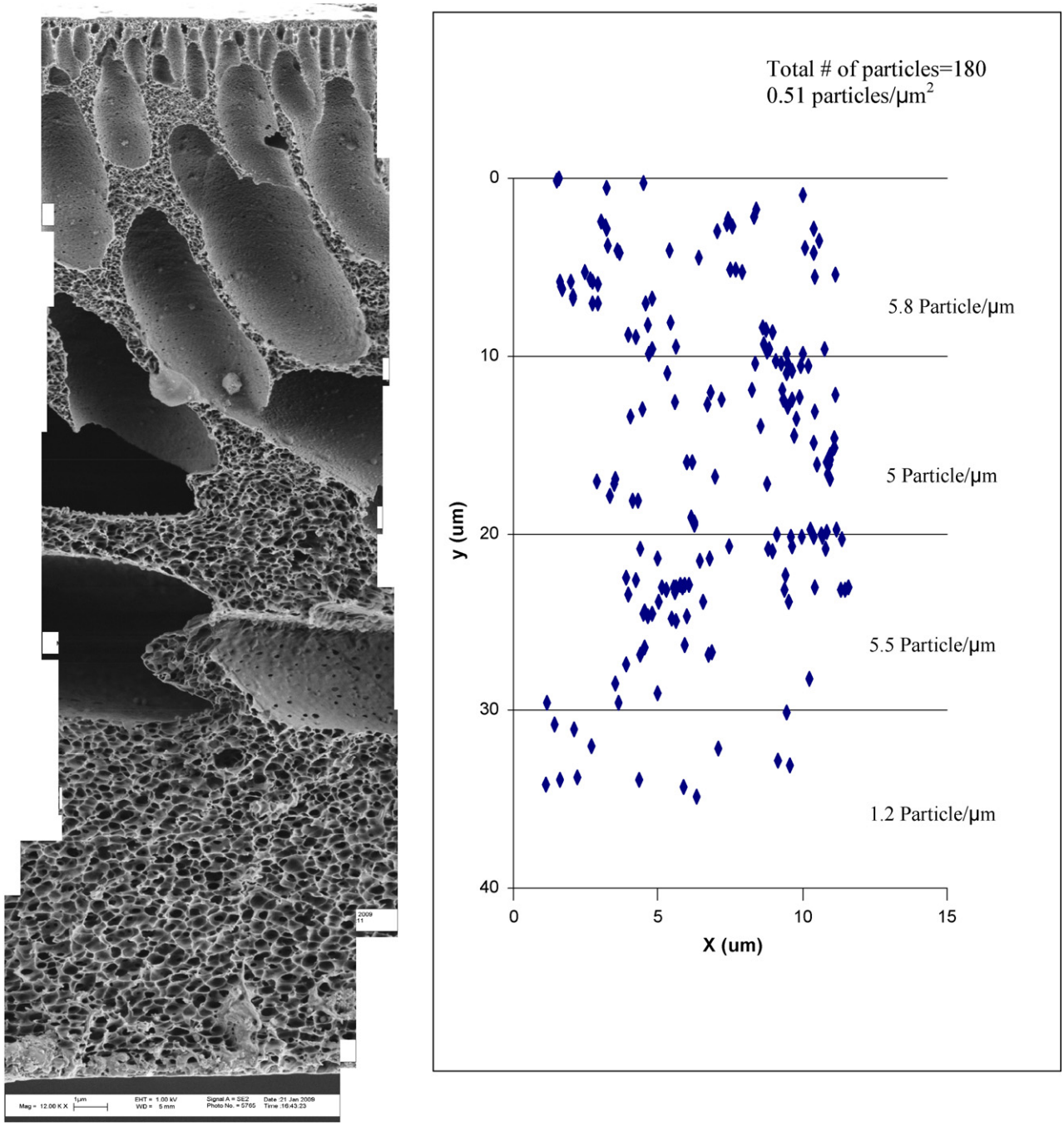

Fig. 4. The Al_2O_3 distribution pattern in 0.03 Al_2O_3/PES.

respectively 1.11×10^7 and 1.13×10^7 m^{-1} despite the tremendous difference in particle density indicates that the pore resistance is not proportional to particle density.

3.3. Membrane fouling evaluation

3.3.1. Flux decline

Fig. 6 illustrates the temporal flux decline for PES and Al_2O_3-entrapped PES membranes using sludge as a feed at 20 °C and TMP of 0.69 bar. Results presented in this paper correspond to an average of two to four replicate with the membranes tested randomly chosen from different independent sheets. Fig. 6 shows that the Al_2O_3-entrapped membranes have higher initial fluxes than the PES membrane. It is important to emphasize that all the observed differences between the four different membrane fluxes were statistically significantly at the 95% confidence level. These results are consistent with the findings of Bae and Tak [38], who found that TiO_2 entrapped PES membranes showed higher flux for sludge filtration than neat polymeric membrane.

Fig. 7a–d illustrates the experimental and theoretical permeability data for tested membranes for sludge filtrations. The theoretical curves were generated by using Sigma Plot software version 10 (Systat Software, Inc., Canada). The data fit the exponential decay (three-parameters) equation (Eq. (1)) with R^2 = 0.94–0.99

$$y = y^{\circ} + ae^{-bt} \quad (1)$$

where y = permeability (L/m^2 bar-h), t = time (h), y° = permeability at (t) equal infinity and a, b are the regression constants. The fouling

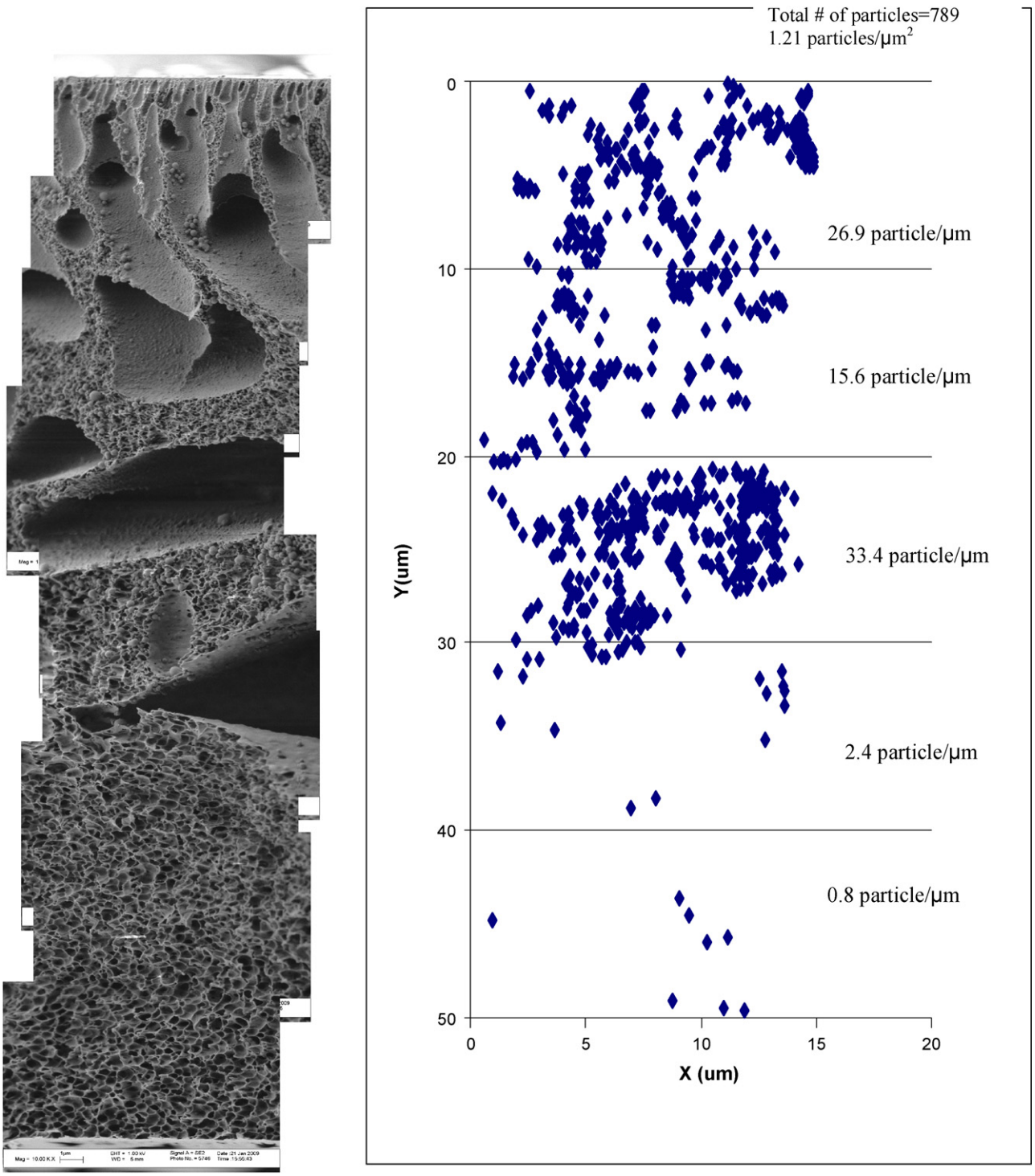

Fig. 5. The Al_2O_3 distribution pattern in 0.05 Al_2O_3/PES.

rate was determined using the following equation

$$\frac{dy}{dt} = abe^{-bt} \quad (2)$$

As apparent from the graphs, the permeability decline for both membranes can be divided into two phases: an initial phase (phase-I) characterized by a rapid decline in permeability followed by a pseudo steady-state phase (phase-II) with a slow permeability decline. This observation is consistent with the hypothetical three-phase-process-mechanisms for initial cake layer formation described elsewhere [39]. The initial and final fouling rates for sludge filtrations by the tested membranes as well as the y° values are shown in Table 6. The initial fouling rates (representing the initial curve) for all membranes are the averages of dy/dt at five points at times varying between 0.01 and 0.05 h. However, the final fouling rates are the averages of dy/dt at five points at times varying between 2.5 and 3 h. It is noteworthy that all the observed differences in fouling rates between the two phases for each membrane were statistically significantly at the 95% confidence level. Furthermore, the differences in phase-I and phase-II fouling rates between

Table 6
Initial and pseudo steady-state fouling rates.

Parameters	PES	0.01 Al_2O_3/PES	0.03 Al_2O_3/PES	0.05 Al_2O_3/PES
Initial fouling rate (L/m^2 bar-h^2)	526.2	2647.3	3301	4387
Pseudo steady-state fouling rate (L/m^2 bar–h^2)	0.005	9.09E−06	6.06E−07	1.25E−11
Pseudo steady-state permeability (y°) (L/m^2 bar-h)	20.4	166	202	252

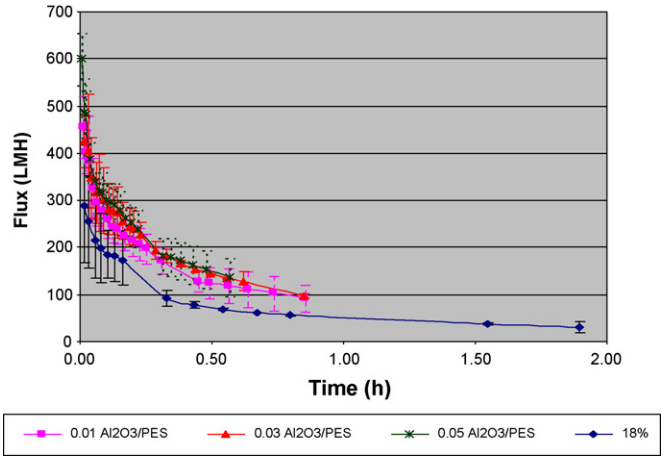

Fig. 6. Temporal flux decline for sludge sample at 0.69 bar.

the tested membranes are also statistically significant at the 95% confidence levels.

As apparent from Table 6, despite the higher initial fouling rate, the steady-state fouling rates of Al_2O_3 entrapped membranes were significantly lower (by 550 times for 0.01 Al_2O_3/PES and 4×10^8 times for 0.05 Al_2O_3/PES membranes) than the neat PES membrane. It is well known that membrane fouling can be influenced by hydrodynamic conditions, such as permeation drag and back transport, and chemical interaction between foulants and membranes [40–42]. Since all the membranes were tested at the same hydrodynamic condition, the different fouling behavior could be attributed to surface properties of the membranes which were changed by nanoparticle entrapment. The surface of Al_2O_3 entrapped membrane can be more hydrophilic than the neat polymeric membrane due to the higher affinity of metal oxides to water. Therefore, hydrophobic adsorption between sludge particle and Al_2O_3 entrapped membrane was reduced. This is further sup-

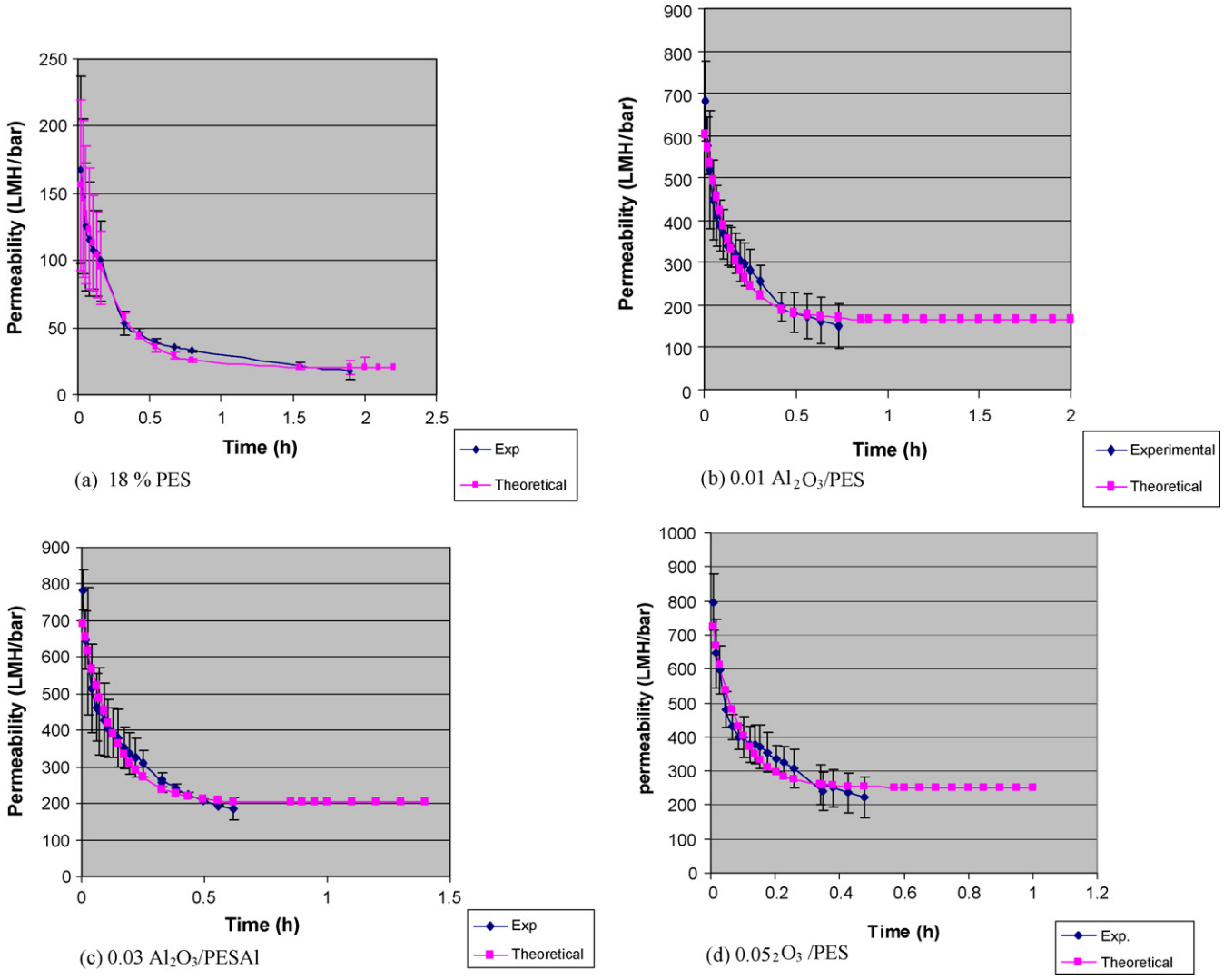

Fig. 7. Membranes permeabilities. (a) 18% PES; (b) 0.01 Al_2O_3/PES; (c) 0.03 Al_2O_3/PES; (d) 0.05 Al_2O_3/PES.

Table 7
Filtration resistances of neat and Al_2O_3 entrapped membranes.

Membrane	R_m ($\times 10^7$) m^{-1}	R_f ($\times 10^7$) m^{-1}	R_c ($\times 10^7$) m^{-1}	R_t ($\times 10^7$) m^{-1}	R_c/R_t%
PES	0.34	1.13	6.2	7.6	81.6
0.01 Al_2O_3/PES	0.38	1.11	0.73	2.22	33
0.03 Al_2O_3/PES	0.39	0.79	0.61	1.79	34
0.05 Al_2O_3/PES	0.32	1.16	0.32	1.8	18

ported by the higher pseudo steady-state permeability (Table 6) observed for the Al_2O_3 entrapped membrane (8–12 times higher) than the neat membrane. Since 0.05 Al_2O_3/PES membranes have the lowest pseudo steady-state fouling rate and the highest pseudo steady-state permeability (Table 6), it is deemed that 0.05 nanoparticles/PES load is the best metal oxide load within the three tested loads.

Despite the relatively different Al_2O_3 distribution pattern between the 0.03 and 0.05 Al_2O_3/PES-membranes (Section 3.2), the performance in terms of change of the membrane permeability with time was similar, Fig. 7c and d. There is no evidence whether the change in Al_2O_3 particles load or the particles distribution pattern inside the membrane matrix is the reason for the difference in pseudo steady-state fouling rate observed between the 0.03 and 0.05 Al_2O_3/PES membranes (Table 6).

3.3.2. *Fouling mitigation of Al_2O_3 entrapped membranes*

The various filtration resistances shown in Table 7 reflect the impact of surface properties on cake layer resistance, with the differences between membrane resistances (R_m) statistically insignificant at the 95% confidence level. The results clearly show that R_c and R_t values decreased substantially with increasing Al_2O_3 load, which coupled with the insignificant differences observed between the R_m values for all tested membranes and also the insignificant differences between R_f values at 95% confidence level (except for 0.03 Al_2O_3/PES membranes) suggests that introducing the Al_2O_3-nanoparticles might enhance PES membrane hydrophilicity. This is further supported by the R_c/R_t ratio (Table 7), which decreased from 82% in the PES to 18% in the 0.05 Al_2O_3/PES attributable to the reduction in hydrophobic interaction between the hydrophobic membrane (PES) and foulants. As apparent from Table 7, the addition of Al_2O_3 reduced the cake resistance (R_c) as well as the R_c/R_t% values, which coupled with the fact that cake resistance mainly due to extracellular polymeric resistance [43] proved to be the predominant fouling mechanism suggests that introducing the Al_2O_3 nanoparticles decrease the adhesion or the adsorption of the EPS on the membrane surface. Bae and Tak [17] concluded that fouling mitigation also increased when the TiO_2 entrapped-nanoparticle content increased in the polysulfone (PSF) casting solution.

4. Conclusions

Al_2O_3 entrapped-PES UF membranes were prepared and applied to activated sludge filtration. Major findings from this study are:

1. Within the 5–20 wt% polymer concentration, the 18% was the optimum. Similarly within the 15–120 s solvent evaporation times, the optimum was found to be 15 s.
2. PES membrane characteristics were changed by the addition of Al_2O_3 nanoparticles to the casting solution, with porosity increasing and the hydrophobic interaction between the membrane surface and foulants decreasing.
3. Al_2O_3 entrapped membrane showed lower flux decline compared to neat polymeric membrane, with the pseudo steady-state permeability increasing by 8- to 12-folds.
4. No relation between the Al_2O_3 particles distribution pattern inside the membrane matrix and the membrane performance could be concluded.
5. Within the 0.01, 0.03 and 0.05 Al_2O_3/PES ratios, the 0.05 was deemed to be optimum in terms of membrane fouling.

Acknowledgement

The authors would like to thank Solvay Advanced Polymers, Alpharetta, GA, USA for supplying the PES polymer.

References

[1] L. Ming-Liang, Z. Jian-Qing, T. Wu, P. Chun Sheng, Hydrophilic modification of poly (ethersulfone) ultrafiltration membrane surface by self-assembly of TiO_2 nanoparticles, Appl. Surf. Sci. 249 (2005) 76–84.
[2] J. Pieracci, J.V. Crivello, G. Belfort, Increasing membrane permeability of UV modified poly(ether sulfone) ultrafiltration membranes, J. Membr. Sci. 202 (2002) 1–16.
[3] F.G. Wilhelm1, I.G.M. Pünt, N.F.A. Van Der Vegt, Cation permeable membranes from blends of sulfonated poly(ether ketone) and poly(ether sulfone), J. Membr. Sci. 199 (2002) 167–176.
[4] I.C. Kim, J.G. Choi, T.M. Tak, Sulfonated polyethersulfone by heterogeneous method and its membrane performance, J. Appl. Polym. Sci. 74 (1999) 2046–2055.
[5] M.L. Steen, A.C. Jordan, E.R. Fisher, Hydrophilic modification of polymeric membranes by low temperature H_2O plasma treatment, J. Membr. Sci. 204 (2002) 341–357.
[6] Y. Yanan, W. Peng, Preparation and characterizations of new PS/TiO_2 hybrid membranes by sol–gel process, Polymer 47 (2006) 2683–2688.
[7] Z.S. Wang, T. Sasaki, M. Muramatsu, Y. Ebina, T. Tanake, L. Wang, M. Watanabe, Self-assembled multilayers of titania nanoparticles and nanosheets with polyelectrolytes, Chem. Mater. 15 (2003) 807–812.
[8] R. Molinari, M. Mungari, E. Drioli, A.D. Paola, V. Loddo, L. Palmisano, M. Schiavello, Study on a photocatalytic membrane reactor for water purification, Catal. Today 55 (2000) 71–78.
[9] R. Molinari, C. Grande, E. Drioli, L. Palmisano, M. Schiavello, Photocatalytic membrane reactors for degradation of organic pollutants in water, Catal. Today 67 (2001) 273–279.
[10] R. Molinari, L. Palmisano, E. Drioli, M. Schiavello, Studies on various reactors configurations for coupling photocatalysis and membrane process in water purification, J. Membr. Sci. 206 (2002) 399–415.
[11] A. Bottino, G. Capannelli, V. D'Asti, et al., Preparation and properties of novel organic–inorganic porous membranes, J. Sep. Purif. Technol. 22–23 (2001) 269–275.
[12] A. Bottino, G. Capannelli, A. Comite, Preparation and characterization of novel porous PVDF–ZrO_2 composite membranes, J. Desalination 146 (2002) 35–40.
[13] Lu. Yan, Y.-S. Li, C.B. Xiang, S. Xianda, Effect of nano-sized Al_2O_3-particle addition on PVDF ultrafiltration membrane performance, J. Membr. Sci. 276 (2006) 162–167.
[14] D.J. Lin, C.L. Chang, F.M. Huang, L.P. Cheng, Effect of salt additive on the formation of microporous poly(vinylidene fluoride) membranes by phase inversion from $LiClO_4$/water/DMF/PVDF system, Polymer 44 (2003) 413–422.
[15] S.Y. Kwak, S.H. Kim, S.S. Kim, Hybrid organic/inorganic reverse osmosis (RO) membrane for bactericidal anti-fouling. 1. Preparation and characterization of TiO_2 nanoparticle self-assembled aromatic polyamide thin film composite (TFC) membrane, Environ. Sci. Technol. 35 (2001) 2388–2394.
[16] S.H. Kim, S.Y. Kwak, B.H. Sohn, T.H. Park, Design of TiO_2 nanoparticle self-assembled aromatic polyamide thin-film-composite (TFC) membrane as an approach to solve biofouling problem, J. Membr. Sci. 211 (2003) 157–165.
[17] T.H. Bae, T.-M. Tak, Effect of TiO_2 nanoparticles on fouling mitigation of ultrafiltration membranes for activated sludge filtration, J. Membr. Sci. 249 (2005) 1–8.
[18] J.M. Duval, B. Folkers, M.H.V. Mulder, G. Desgrandchamps, C.A. Smolders, Adsorbent filled membranes for gas separation. Part 1. Improvement of the gas separation properties of polymeric membranes by incorporation of microporous adsorbents, J. Membr. Sci. 80 (1993) 189–198.
[19] M. Moaddeb, W.J. Koros, Gas transport properties of thin polymeric membranes in the presence of silicon dioxide particles, J. Membr. Sci. 125 (1997) 143–163.
[20] C.M. Zimmerman, A. Singh, W.J. Koros, Tailoring mixed matrix composite membranes for gas separations, J. Membr. Sci. 137 (1997) 145–154.
[21] I.F.J. Vankelecom, S. DeBeukelaer, J.B. Uytterhoeven, Sorption and pervaporation of aroma compounds using zeolite-filled PDMS membranes, J. Phys. Chem. B 101 (1997) 5186–5190.

[22] J.P. Boom, I.J.M. Pünt, H. Zwijnenberg, R. de Boer, D. Bargeman, C.A. Smolders, H. Strathmann, Transport through zeolite filled polymeric membranes, J. Membr. Sci. 138 (1998) 237–258.
[23] X. Chen, Z.H. Ping, Y.C. Long, Separation properties of alcohol–water mixture through silicalite-I-filled silicone rubber membranes by pervaporation, J. Appl. Polym. Sci. 67 (1998) 629–636.
[24] I. Genne, W. Doyen, W. Adriansens, R. Leysen, Organo-mineral ultrafiltration membranes, Filtr. Separat. 34 (1997) 964–966.
[25] T. Matsuura, Synthetic Membranes and Membrane Separation Processes, CRC Press, Boca Raton, FL, 1994.
[26] T. Ueda, K. Hata, Domestic wastewater treatment by a submerged membrane bioreactor with gravitational filtration, Water Res. 33 (1999) 2888–2892.
[27] X. Zheng, J. Liu, Dyeing and printing wastewater treatment using a membrane bioreactor with a gravity drain, Desalination 190 (2006) 277–286.
[28] X. Zheng, J.X. Liu, Optimizing of operational factors of a membrane bioreactor with gravity drain, Water Sci. Technol. 52 (2005) 409–416.
[29] B. Fan, X. Huang, Characteristics of a self-forming dynamic membrane coupled with a bioreactor for municipal wastewater treatment, Environ. Sci. Technol. 36 (2002) 5245–5251.
[30] S. Arabi, G. Nakhla, Impact of calcium on the membrane fouling in membrane bioreactors, J. Membr. Sci. 314 (2008) 134–142.
[31] M. Mulder, Basic Principles of Membrane Technology, Kluwer Academic Publishers, 1996, p. 383.
[32] M.I. Mustaffar, A.F. Ismail, R.M. Illias, Study on the effect of polymer concentration on hollow fiber ultrafiltration membrane performance and morphology, in: Regional Symp. Membrane Science and Technology, 2004.
[33] S.C. Pesek, W.J. Koros, Aqueous quenched asymmetric polysulfone hollow fibers prepared by dry/wet phase separation, J. Membr. Sci. 88 (1994) 1–19.
[34] G. Pei, G. Cheng, Q. Du, Preparation of chelating resin filled composite membranes and selective adsorption of Cu(II), J. Membr. Sci. 196 (2002) 85–93.
[35] R.C. Bindal, M.S. Hanra, B.M. Misra, Novel solvent exchange cum immersion precipitation technique for the preparation of asymmetric polymeric membrane, J. Membr. Sci. 118 (1996) 23–29.
[36] X. Jian, Y. Dai, G. He, G. Chen, Preparation of UF and NF poly (phthalazine ether sulfone ketone) membranes for high temperature application, J. Membr. Sci. 161 (1999) 185–191.
[37] I.C. Kim, K.H. Lee, T.M. Tak, Preparation and characterization of integrally skinned uncharged polyetherimide asymmetric nanofiltration membrane, J. Membr. Sci. 183 (2001) 235–247.
[38] T.H. Bae, T.-M. Tak, Interpretation of fouling characteristics of ultrafiltration membrane during the filtration of membrane bioreactor mixed liquor, J. Membr. Sci. 264 (2005) 151–160.
[39] S.P. Hong, T.H. Bae, T.M. Tak, S. Hong, A. Randall, Fouling control in activated sludge submerged hollow fiber membrane bioreactor, Desalination 143 (2002) 219–228.
[40] E. Tardieu, A. Grasmick, V. Geaugey, J. Manem, Hydrodynamic control of bioparticle deposition in a MBR applied to wastewater treatment, J. Membr. Sci. 147 (1998) 1–12.
[41] E. Tardieu, A. Grasmick, V. Geaugey, J. Manem, Influence of hydrodynamics on fouling velocity in a recirculated MBR for wastewater treatment, J. Membr. Sci. 156 (1999) 131–140.
[42] W.T. Lee, S.T. Kang, H.S. Shin, Sludge characteristics and their contribution to microfiltration in submerged membrane bioreactors, J. Membr. Sci. 216 (2003) 217–227.
[43] N. Maximous, S. Arabi, M. Kim, G. Nakhla, Comparison of biofoulants in BNR-MBR and conventional MBR (C-MBR) systems, in: WEFTEC conference, October 18–22, McCormick Place Chicago, IL, 2008.